

# Fractal Concepts for Antenna Design and Analysis

K. J. VINOY

Department of Electrical Communication Engineering, Indian Institute of Science Bangalore 560012.

## ABSTRACT

Fractal geometries have several interesting properties and therefore are of high interest in many fields of science and engineering. In recent years many practical antennas with these geometries have been developed for several wireless applications. Such antennas often have reduced size and multi-frequency characteristics. This article summarizes efforts to relate mathematical properties of fractals in designing and analyzing the behaviour of antennas using them.

**Keywords:** Wireless antennas, Fractal antennas, dipole antennas, microstrip antennas, multi-frequency antennas, multi-port network model.

## 1 INTRODUCTION

The use of fractal geometries has significantly impacted many areas of science and engineering including the design and analysis of microwave antennas. Antennas using some of these geometries have already been developed for various telecommunications applications. These geometries have been shown to improve several antenna features to varying extents. The term fractal was coined by Mandelbrot during 1970's after his pioneering research on several naturally occurring irregular and fragmented geometries that are not contained within the realms of conventional Euclidian geometry [Mandelbrot (1983)].

Some examples of fractals used in antenna engineering are given in Fig. 1. These are irregular in nature, and are infinitely sub-divisible with each division a copy of the parent. These have several interesting features uncommon with Euclidean geometries. Fractals are known to have non-integer values for their dimension. Dimension of a geometry can be defined in several ways, but the most easily understood definition is that for self-similarity dimension. To obtain this value, the geometry is divided into scaled down, but identical copies of itself. If there are  $n$  such copies of the original geometry scaled down by a fraction  $f$ , the similarity dimension  $D$  is defined as:

$$D = \frac{\log n}{\log(1/f)} \quad (1)$$

The same approach can be followed for determining the dimension of fractal geometries as shown in Fig. 1 and are listed in Table 1.

Although this approach is very convenient for many such geometries, all fractals are not amenable for this approach. Such is the case with most plane-, or space-filling fractals. In these cases Hausdorff dimension or any other mathematically intensive definitions of dimension would be required.

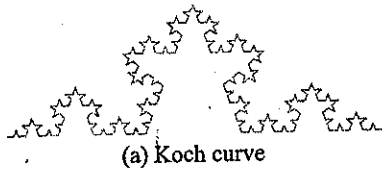
Table 1 Fractal dimension of geometries shown in Fig. 1

Geometry	Dimension
Koch curve	1.2619
Sierpinski gasket	1.5850
Sierpinski carpet	1.893
Minkowski curve	1.465

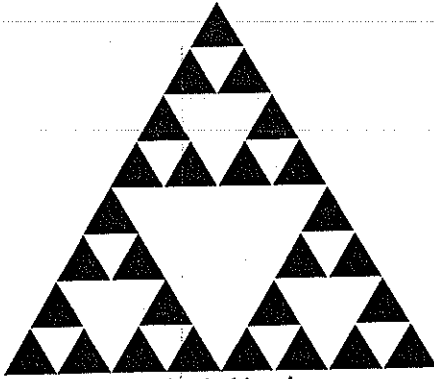
Non-integer dimension is not the only special property of fractals. Many fractal geometries are self-similar, a property which makes it easier to accurately compute their Hausdorff dimension. In order to define self-similarity mathematically, first the concept of contraction is introduced. A map  $\psi : \mathbf{R}^n \rightarrow \mathbf{R}^n$  is a contraction if there exists some constant number  $c \in (0, 1)$  so that the inequality [Kaye (1994)]

$$\|\psi(x) - \psi(y)\| \leq c \|x - y\| \quad (2)$$

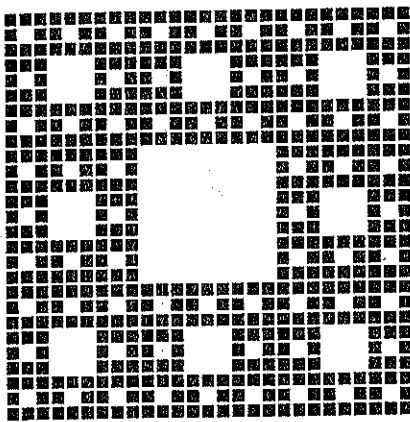
holds for any  $x, y \in \mathbf{R}^n$ . For a natural number  $m \geq 2$ , and a set of  $m$  contractions  $\{\psi_1, \psi_2, \dots, \psi_m\}$  defined on  $\mathbf{R}^n$ , a non-empty compact set  $V$  in  $\mathbf{R}^n$  is self-similar if



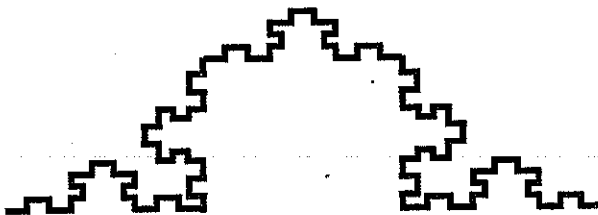
(a) Koch curve



(b) Sierpinski gasket



(c) Sierpinski carpet



(d) Minkowski curve

Fig.1 Some common examples of fractals used in antenna engineering

$$V = \bigcup_{i=1}^m \psi_i(V) \tag{3}$$

Each such division of the geometry is termed an iteration. Fractal geometries are generally infinitely sub-divisible. Self similar sets defined by linear contractions are called self-affine sets. Other properties associated with fractal geometries include scale-invariance, plane-filling or space-filling nature,

and lacunarity. Lacunarity is a term coined to express the nature of area fractal having hollow spaces ("gappiness") [Falconer (1990)].

Like dimension of fractals, their lacunarity has also been defined and characterized in several ways. An object is said to have high lacunarity if it has clustered holes, intervals or voids. Lacunarity is therefore interpreted as a measure of the lack of rotational or translational invariance of an image [Mandelbrot (1982); Wu (1988)]. In a broader sense, it is a measure of the degree of heterogeneity within an object. There are a number of measures suggested in literature for expressing lacunarity. But most of these methods are structure-specific and do not have a wide general applicability. Lacunarity is usually defined from the mass-related distribution. In the box-counting method, the D-dimensional measure in each box of side  $r$  can be written in the form [Cheng (1997)].

$$M(r) = A(r)r^D \tag{4}$$

with the restriction  $\log A/\log r \rightarrow 0$ . In eq. (3.1)  $A(r)$ , in general, is a function of  $r$  and  $M(r)$  is the mass in a box of size  $r$ .

Lacunarity can, therefore, be quantitatively defined as the fluctuations of mass-distributions over its mean. It is thus, given by [Allain and Cloitre (1991)]:

$$\Lambda(r) = \frac{E\{M^2(r)\}}{E^2\{M(r)\}} \tag{5}$$

where  $E(x) = \text{Expectation}(x)$

The above definition of lacunarity can be expressed in terms of the first and second moments of spatial distribution as:

$$\Lambda(r) = \frac{Z^{(2)}(r)}{[Z^{(1)}(r)]^2} \tag{6}$$

The first and second moments of the distribution are given by

$$Z^{(1)}(r) = \sum_M MP(M, r) \tag{7}$$

$$Z^{(2)}(r) = \sum_M M^2 P(M, r) \tag{8}$$

Although the lacunarity depends on the box size, a unique value independent of this can be obtained by for the same by various ways. Recently we have proposed an approach that works for fractals with different fractal dimensions [Sengupta and Vinoy

(2006)] and this has been found to be of interest in fields such as image edge detection and pattern recognition [Berthe and Vinoy (2011); Kilic and Abiyev (2011)]. In the following sections a brief overview is provided on the use of these fractal properties in antenna design and analysis.

## 2. FRACTAL FEATURES IN ANTENNA DESIGN

Some of the common examples of planar antenna geometries are printed dipoles, monopoles, loops, and patches. Various shapes of geometries (regular and fractal) have been used in all these types. Most of these are resonant antennas, in which one of the critical dimensions (length for dipoles and monopoles, perimeter for loop and a side for a rectangular patch) decide the operational frequency of the antenna. Therefore, size reduction for linear antennas with highly iterated fractal geometries can be easily understood. This property has been used in designing fractal antennas for low frequency wireless applications such as in RFID tags.

Another important antenna characteristics common with fractal-shaped antennas is their multi-frequency behaviour [Werner *et al* (1999)]. Often this is linked to the self-similarity of the geometry. Compared to other irregular geometries, the use of fractals brings in a kind of mathematical order into the antenna shape; the effectiveness and the use of such an order can therefore be explored. As a first step in this direction, the design equations for dipole antenna using Hilbert curves have been obtained in terms of their geometrical parameters [Vinoy *et al* (2001a)]. But more systematic relationships between antenna characteristics and quantifiable fractal features such as dimension and lacunarity can be observed by studying some generalizations of Koch curves in Fig 1a. These generalizations resulted in varying mathematical properties for the generic geometry (indentation angle), which could then be related to antenna characteristics. Dipole antennas with these have two geometries in the figure, with a feed generally at the centre of the completed geometry.

Fractal dimension of the generalized Koch curve depends on the indentation angle, and that the antenna properties can be linked to the indentation angle of the Koch curve geometry. The fractal dimension of this

geometry changes from 1 (dimension of a straight line) to the maximum value of 2 (dimension of plane), as the angle is increased from 0 to 90°. A simulation study of the performance of these dipole antennas, showed that the input characteristics change significantly by these modifications. The results presented in Fig.2 establish a direct correspondence between the fractal dimensions of the geometry and the performance of the antennas constructed using them. It is therefore possible to obtain a design equation for this type of antenna using the order of fractal iteration  $n$  and the dimension  $D$  of the geometry as inputs. Using a curve fitting approach, to fit the parametric curves in Fig.2, we get [Vinoy (2001); Vinoy *et al*, (2003)]

$$f_K = f_D \left[ 1 - \exp\left(\frac{n-1}{n} \frac{\ln D}{D}\right) \right] \quad (9)$$

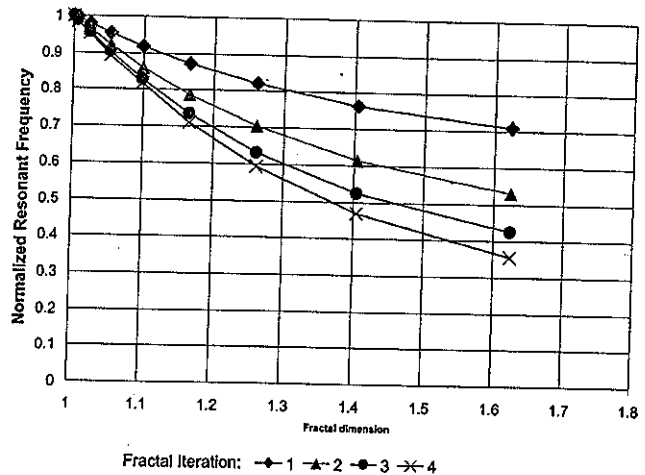


Fig.2. The normalized resonant frequency of generalized Koch dipole antennas of different fractal iterations

where  $f_D$  is the resonant frequency of the linear dipole antenna with the same (end-to-end) length as the Koch curve. Curves are shown for various iteration geometries shown in Fig.3(a)-(c). The fractal dimension of these changes as we change the indentation angle. Multiple resonant frequencies of a fractal element antenna using Koch curves have also been similarly related to the fractal dimension of the geometry.

In an effort to generalize this even further, during a recent project work we explored an approach to construct fractal geometries that are not self-similar. One such geometry is shown in Fig.3(d). Taking in Hausdorff dimension  $D_f$  and lacunarity parameter  $\bar{\Lambda}$  and normalizing the resonant frequency with respect

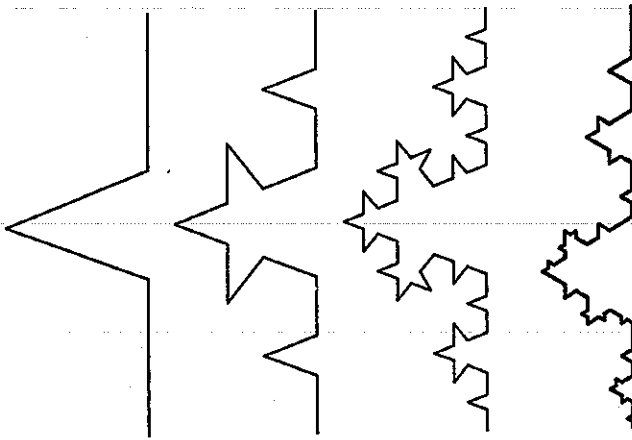


Fig.3. Various geometries of Koch curves (a) iteration 1, (b) iteration 2, (c) iteration 3, and (d) 3rd iteration geometry without self-similarity

to that of a linear dipole with the same end-to-end length as the Koch curve, we obtained the resonant frequency of dipoles with these generalized geometries by curve fitting as [Sengupta and Vinoy (2006)]

$$f_r = \frac{f_d}{\exp(\bar{\Lambda}_d^{0.769})} \left[ 1 - 0.67 \left( \frac{\ln D_f}{D_f} \right)^2 \right] \exp(\bar{\Lambda}^{0.769}) \quad (10)$$

where  $f_d = 720.2$  MHz and  $\bar{\Lambda}_d = 2.789$  are the primary resonant frequency and the lacunarity, respectively, of the linear dipole antenna.

A comparison of the predicted values of the resonant frequencies and the values obtained using NEC are presented in Fig.4. The RMS error in prediction using eq (10) is only 0.8%. The figure also

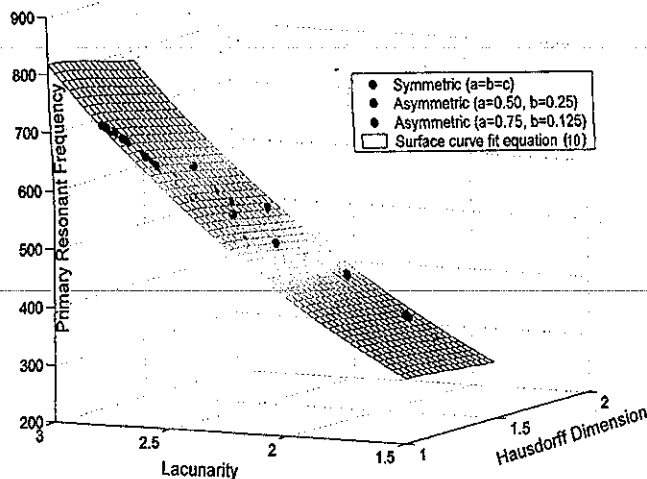


Fig.4. Resonant frequency of Koch dipole antennas calculated with Eq. (10) and numerical simulations

reveals a very strong dependence of dipole antenna behaviour with lacunarity and weaker correlation with fractal dimension. Neglecting the effect of dimension and keeping the dependence form similar to Eq. (10), we get the following curve fit

$$f_r = \frac{f_d}{\exp(\bar{\Lambda}_d^{0.8})} \exp(\bar{\Lambda}^{0.8}) \quad (11)$$

This curve-fit gives an RMS error of only 1.05%. This simple expression in Eq. (11) encompasses all symmetric and asymmetric variants of Koch dipoles and is a function of a single variable which is lacunarity.

Due to the presence of a large number of closely placed line segments, antennas using geometries such as Hilbert curves can be designed for reconfigurable radiation characteristics with the inclusion of few additional line segments and RF switches [Vinoy *et al* (2001b) Vinoy and Varadan (2001)]. Although these switch positions are not optimized for specific performance, they offer immense potential for designing antennas with novel characteristics.

### 3. Exploiting Fractal Features in Antenna Analysis

Although the size reduction and multi-frequency characteristics of dipole and other linear antennas are widely appreciated, these non-conformal antennas have limited use in many applications. Microstrip antennas, despite having low bandwidth, have become popular in the last quarter of the 20th century precisely for their planar and conformal characteristics. Hence we have studied microstrip patch and ring antennas with some fractal profiles. We found that by suitably choosing the pre-fractal geometries for the sides of ring antennas, they can be designed for multi-band operation. Unlike regular geometries we studied, the fractal shape resulted in similar radiation characteristics at all bands of operation.

In a recent effort, a ring microstrip radiator excited by microstrip transmission line feed, in which one or more arms replaced by fractal Minkowski curves as shown in Fig.5 have been studied. The resonant frequencies of such antennas are decided by the electrical perimeter of the ring geometry used. It is therefore obvious that by using fractal geometries such as Minkowski curves in Fig.5 (c) and (d) the resonant

frequencies can be lowered. In other words, antenna size can be reduced by this approach.

In our research, we generalized configurations in Fig.5 (c) and (d) as we did for self-similar Koch dipoles, and found that the reduction in resonant frequency is similar for both these geometries. However, the antenna using geometry in Fig.5(d) was found to have dual frequency characteristics. Even the antenna in Fig.5(c) resonates at the same frequency as the other, but the radiation characteristics of this antenna is not suitable at the second resonant frequency. Furthermore, we have reported basing on the parametric studies that such dual-frequency characteristics of the antenna tend to improve as the underlying geometry approaches self-similarity [Vinoy and Pal (2010)].

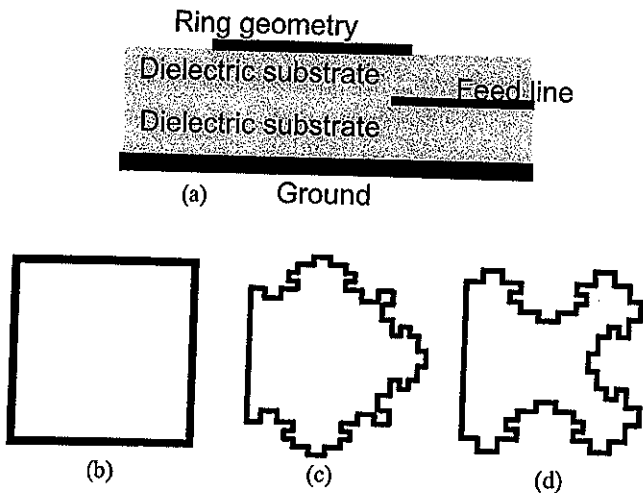


Fig.5. Square ring antenna (a) cross sectional view and (b)-(d) Top views: (b) square geometry (c) and (d) two approaches of replacing straight segments with second iteration fractal Minkowski curves

Although the antenna size is reduced when fractal geometry is used here, the bandwidth also follows suit, affecting their practical use. In a parallel study we have found that ring geometries with non-uniform width tend to have better bandwidth than those with uniform width [Behera and Vinoy (2009)]. In these square ring antennas, the width of two sides parallel to the feed arm is increased to improve bandwidth. This may pose a problem if incorporated with the Minkowski ring antennas with three fractal geometries. Hence we have attempted a geometry shown in Fig.6 to design an antenna with both dual frequency characteristics and reasonable bandwidths at these frequencies. The feed to this ring geometry is through

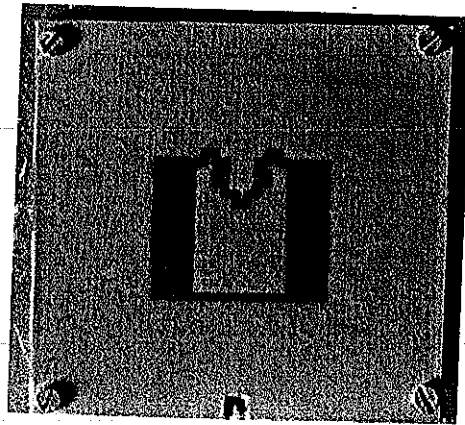


Fig.6. Fabricated dual band antenna

a transmission line on a separate dielectric layer below that for the geometry.

In order to assess the effectiveness of various sub-parts of this antenna geometry, we have analyzed this by dividing the geometry into several segments of rectangular shape. This approach of dividing a geometry to analyze the behaviour was put forward by Professor KC Gupta several years ago [Gupta (1989)]. This approach is known as the multi-port network modelling. For example, the antenna with the first iteration geometry may be divided into eight segments of regular shapes as shown in Fig.7. These geometries may be connected with a total of sixteen interconnecting ports and an additional input port for the antenna feed. There are nine equations for voltages and co-joined all voltages appeared in vector matrix.

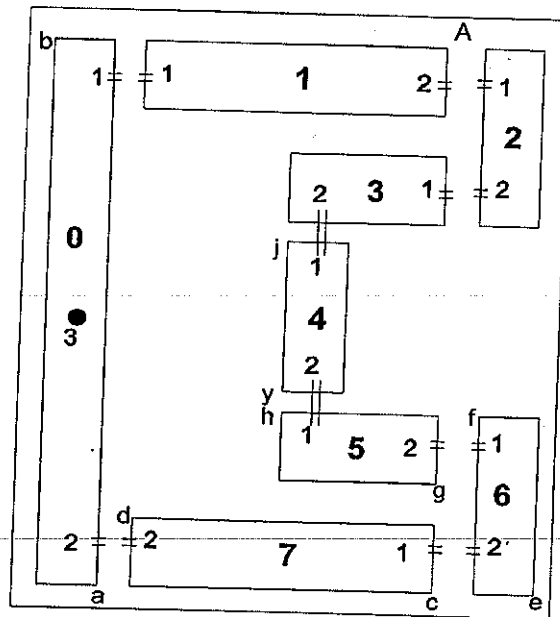


Fig.7 Segmentation of Square ring microstrip antenna with one side replaced by fractal geometry at first iteration

In this approach, each segment has two end ports (i.e. 1 and 2). The voltage, current and impedance at port  $m$  of segment number  $n$  can be written as,  $V_{n_m}$ ,  $I_{n_m}$  and  $Z_{n_m}$  respectively. In the geometry in Fig.7, the self and mutual impedances are computed using Green's functions. Using these impedances, the voltage and current equations for the geometry can be written in general form as

$$V_{n_1} = Z_{n_{11}} I_{n_1} + Z_{n_{12}} I_{n_2} \quad (12)$$

$$V_{n_2} = Z_{n_{22}} I_{n_2} + Z_{n_{21}} I_{n_1} \quad (13)$$

where  $n = 1$  to 7 representing segment numbers, as shown in the above figure. Subscripts 1 and 2 in the above expressions are denoting inter-connected port numbers of the corresponding segment. The expressions for the 0<sup>th</sup> segment relate voltages and currents at three ports on the segment. The impedance terms can be evaluated using planar Green's functions.

We can impose the boundary conditions by enforcing continuity of current and voltage at interconnecting ports for segments number 1 to 6 as

$$\begin{aligned} V_{n_2} &= V_{(n+1)_1} \\ I_{n_2} &= -I_{(n+1)_1} \end{aligned} \quad (14)$$

Additionally, we can make use of the information that the port 3 is located at the middle of the segment, so that the entire geometry is symmetric about the excitation port. Now, the above seventeen equations can be solved to obtain the input impedance formula of the microstrip fractal ring antenna. This method of joining all the elemental segments can be used to obtain the final expression for the input impedance of irregular microstrip structures. Exploitation of self-similarity of fractal geometry can help reduce the computations even further. In the case of second iteration geometry, a large number of segments have similar orientation and hence the respective impedance terms have identical values. On the other hand the computational accuracy is of the order of 1%.

In order to validate the above analytical results, a prototype antenna was fabricated and tested. The photograph of the prototype antennas fabricated with the physical dimensions of 1mm ring width and the length of the initiator = 21.7 mm. and the indentation factor ( $k$ ) = 1, excited through electromagnetic coupling is shown in Fig.6. The fabricated antenna is

characterized using a vector network analyzer. The return loss characteristics obtained by measurements, simulation and those calculated by the above MNM approach compared well as shown in Fig. 8. A detailed comparison of various antenna parameters for antennas with the first and second iteration fractal geometries are tabulated in Table 2. Antenna performance at the first two resonances are *included here.*

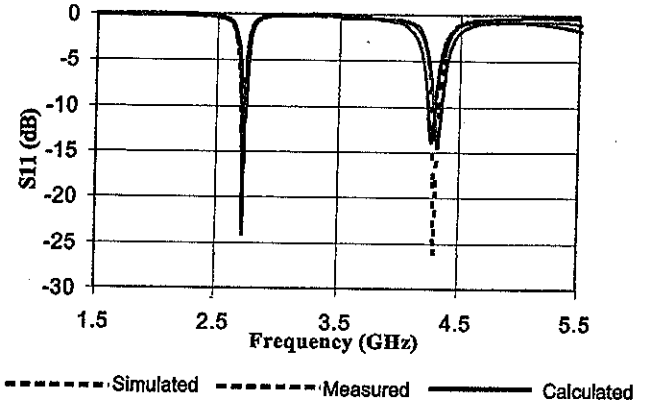


Fig.8 Return loss characteristics of the Fractal Microstrip ring antenna shown in Fig.6

Table 2 Comparison of the simulated and measured performances of the dual-frequency microstrip ring antennas. The dimensions of feed strip ( $l_s, w_s$ ) has been optimized for a good impedance match for each antenna

Antenna Performance	Ring Antenna (1st iteration)	Ring Antenna (2nd iteration)	
	$w_1 = 1\text{mm}, w_2 = 7\text{mm.}$	$w_1 = 1\text{mm}, w_2 = 7\text{mm.}$	
Fr (GHz)			
Simulated	2.95	4.71	2.725 4.275
Fr (GHz)			
Measured	2.945	4.75	2.78 4.298
BW(MHz)			
Measured	35.05	72.2	28.5 60.8
Gain dBi)			
Measured	5.2	4.5	4.45 5.4

These results indicate that the multiport network modelling approach is very effective to analyze fractal antennas. This approach exploits the ordered nature of fractals in simplifying the analysis, and therefore avoids computation redundancy.

#### 4 CONCLUSIONS

1. Fractal geometries may be used to design dual and multi-frequency antennas. In many such instances the behaviour of these dipole and monopole

antennas may be related to the fractal properties of the underlying geometry. Fractal dimension and lacunarity have been found to follow the resonant behaviour of many variations of such antennas.

2. The ordered nature of fractals can also become very useful in the design and analysis of such antennas. It has been found that multi-port network modelling of microstrip antenna can benefit significantly by this. A significant reduction of computations required, without compromising the accuracy would be possible for antennas with self-similar fractal geometries.

## REFERENCES

1. Allain, C; Cloitre, M; (1991) Characterizing the lacunarity of random and deterministic fractal sets, *Phys. Rev. A* 44 3552-3558.
2. Behera S.; Vinoy, K.J.; (2009) Microstrip Square Ring Antenna for Dual-Band operation, *Progress in Electromagnetics Research PIER* 93, pp. 41-56, 2009
3. Berthe K.A.; Vinoy K.J.; (2011) A New Method for Automated Edge Detection using Fractal Properties of Images, submitted to *Int. J. Electronics & Communications*.
4. Falconer, K.J.; (1990) *Fractal Geometry: Mathematical Foundations and Applications*, New York: Wiley.
5. Gupta, K.C.; (1989) Multiport network approach for modelling and analysis of patch antennas and arrays, In: J. R. James and P. S. Hall, *Handbook of Microstrip Antennas*. Peter Peregrinus Ltd., UK, London, Chapter 9.
6. Kaye, B.H.; (1994) *A Random walk through Fractal Dimensions*, New York: VCH.
7. Kilic, L.I.; Abiyev, R.H.; (2011) Exploiting the synergy between fractal dimension and lacunarity for improved texture recognition, *Signal Processing* 91 2332-2344
8. Mandelbrot, B.B.; (1983) *The Fractal Geometry of Nature*, New York: W.H. Freeman.
9. Sengupta, K.; Vinoy, K.J.; (2006) A New Measure of Lacunarity for Generalized Fractals and its Impacts in Electromagnetic Behaviour of Generalized Koch Dipole Antennas, *Fractals* Vol. 14, No. 4, 271-282.
10. Vinoy, K.J.; (2002) Fractal shaped antenna elements for wide- and multi-band wireless applications, Ph.D. Dissertation. Pennsylvania State University.
11. Vinoy, K.J.; Varadan, V.K.; (2001) Design of reconfigurable fractal antennas and RF-MEMS for space-based systems, *Smart Materials and Structures*, vol. 10, pp. 1211-1223, 2001.
12. Vinoy, K.J.; Jose, K.A.; Varadan, V.K.; Varadan, V.V.; (2001a) Hilbert curve fractal antenna: a small resonant antenna for VHF/UHF applications, *Microwave & Optical Technology Letters*, vol. 29, pp. 215-219.
13. Vinoy, K.J.; Jose, K.A.; Varadan, V.K.; Varadan, V.V.; (2001b) Hilbert curve fractal antennas with reconfigurable characteristics, in: *IEEE- MTT International Symposium*, Phoenix May 20-25, 2001, Digest, vol. 1, pp. 381-384.
14. Vinoy, K.J.; Jose, K.A.; Varadan, V.K.; (2004) Impact of fractal dimension in the design of multi-resonant fractal antennas, *Fractals*, vol. 12, pp. 55-66.
15. Vinoy K.J.; Pal, A.; (2010) Dual frequency Characteristics of Minkowski-Square Ring Antennas, *IET Microwaves, Antennas & Propagation*, vol. 4 (2). pp. 219-224.
16. Werner, D.H.; Haupt, R.L.; Werner, P.L. (1999) Fractal antenna engineering: The theory and design of fractal antenna arrays, *IEEE Antennas and Propagation Mag.*, vol. 41, no. 5, pp. 37-59.